Long-term spectral variavation of 3C 66A with Fermi and Kanata Telescope

R. Itoh[1],Y. Fukazawa[1], Kanata Team and the Fermi Large Area Telescope Collaboration

[1] Hiroshima-Univ.
E-mail(RI): itoh@hep01.hepl.hiroshima-u.ac.jp

Abstract

3C 66A is an intermediate-frequency peaked BL Lac object and detected by in the gamma-ray energy band. We reported the long-term GeV gamma-ray and optical observations of 3C 66A using the Fermi Large Area Telescope (LAT) and the Kanata Telescope. We found two types of variations. In 2008, the gamma-ray flux, optical flux, optical color, and optical polarization degree showed a clear correlation. On the other hand, in 2009-2010, the correlation became quite weak; only the optical flux gradually increased. These properties might be explained by the situation that there are two emission regions; one is close to the source of Comptonized seed photons, and the other is distant.

Key words: Black hole

1. Introduction

Blazars are highly variable active galactic nuclei (AGN) observed in all wave-lengths from radio to TeV gamma-ray band. They have a strong relativistic jet aligned with the observer's line of sight and are apparently bright due to the relativistic beaming effect. Their emission typically consists of two components. One is attributed to the synchrotron radiation in the low energy band with high polarization, and the other is the inverse Compton scattering of low enery photons by relativistic electrons.

3C 66A is one of famous TeV blazars, and this source is classified as an IBL (Intermediate-frequency-peaked BL Lac). Its lower-energy spectral component extends from radio to soft X-rays with a peak in the optical band (Abdo et al. 2010a). Most TeV blazars are classified as HBL (High-frequency-peaked BL Lac) or IBL, and therefore 3C 66A is a valuable source to figure out the mechanism of high energy gamam-ray emissions. The higher-energy component is observed from MeV to TeV gamma-ray band, and explained by the Synchrotron Self-Compton (SSC) plus External Compton (EC) model (Abdo et al. 2010d and references therein). Due to its week emission line in the optical band, the redshift is uncertain. Miller et al. (1978) gave the redshift z = 0.444 by Mg II line. However, as pointed out by Bramel et al. 2005, this redshift is still uncertain because it was measured by only a single weak line. The redshift uncertainty affects on correcting the Extragalactic Background Light (EBL) absorption in the TeV gamma-ray band. Because of this problem, the true spectrum in the TeV gamma-ray band is not well known and their emission mechanism is not yet understood. Thererfore, the multi-wavelength observation is powerful to probe the emission mechanism.

The Fermi gamma-ray space telescope has opened a new era of multi-wavelength monitoring observations of AGN. Correlation studies between the GeV gamma-ray and optical band are important since the energy of their emitting electrons is similar. Simultaneous gamma-ray and optical observations have been extensively performed, and in particular, the optical polarimetric observations give a strong tool to probe the jet structure. 3C 66A coincides with an EGRET source 3EG J0222+4253, but there is a gamma-ray pulsar close to 3C 66A and EGRET could not resolve them, and therefore the GeV gamma-ray flux was not obtained accurately. Thanks to better point spread function, Fermi can separate these sources and obtain the GeV gamma-ray flux of 3C 66A accurately for the first time. 3C 66A is listed as 1FGL J0222.6+4302 in the 1st-year Fermi catalog (Abdo et al. 2010b) and newly classied as Intermediate-synchrotron-peaked blazar (ISP) (Abdo et al. 2010a). In this paper, we report correlation studies of GeV gamma-ray and optical emissions, based on the simultaneous observations of 3C 66A by Fermi and Kanata optical telescope.

2. Observations and Results

2.1. *Fermi* observation and Data analysis

The Large Area Telescope (LAT) is the main instrument of *Fermi* Gamma-ray Space Telescope. The LAT is an electron-positron pair production detector which is sensitive to γ rays with energies from 20 MeV to 300 GeV.

LAT observes the whole sky every 3 hour with a large effective area of 8000cm^2, a wide field of View of 2.4 sr, and a high positional resolution 0.1° at 10 GeV. Details are described in Atwood et al. (2009). The data used in this analysis are taken between 2008 August and 2009 September in the sky survey mode. The data were analyzed using the standard *Fermi* analysis software called `Science Tools` (version v9r15, IRFs P6_V3). In order to reduce contamination of backgrounds, only class-3 events (also called "Diffuse", highest quality photon data) were selected for this analysis, and a selection of events with zenith angle <105° was applied to suppress the earth albedo. We performed the *Unbinned Likelihood* analysis to estimate the spectrum and flux of 3C 66A, using `gtlike` packaged in the `Science Tools`. The area of 15 degrees from 3C 66A was selected as a region of interest (ROI) for the analysis. The model includes a point source at the position of 3C 66A and a background component of the Galactic diffuse emission and isotropic diffuse emission. There are some bright source within 15° of 3C 66A, and 6 point sources (B30133+388, QSO DA55, S4 0218+35, J0237+2848, CGRaBSJ0319+4130 and PSR J0218+4232) were also included in the model. They have a TS value of >100 in the 1st-year Fermi catalog (Abdo et al. 2010b). TS is an indicator of the significance of signals from sources corresponding to $TS \simeq \sigma^2$ where σ is a standard deviation. Spectrum model of each point source was constructed by a simple power-law. The model that we adopted for the Galactic component is given by the file `gll_iem_v02.fit`, and the isotropic component, which is the sum of the extragalactic diffuse emission and the residual charged particle background, is parametrized by the file `isotropic_iem_v02.txt`.

In order to obtain a gamma-ray light curve of 3C 66A in the energy band from 100 MeV to 100 GeV, a flux is estimated by the likelihood analysis for the data in every 5 day with a power-law model. The same model was applied for the other sources. The background model parameters representing the spectral shape are fixed and only the normalization is let free. We take an integrated photon flux to derive the light curve for the time bin where the obtained Test Statistics (TS) value is larger than 10, corresponding to the significance of $\sim 3\sigma$. Because of TS selection, some of data points disappear in the light curves.

2.2. Kanata Telescope Observations

We performed the *V*,*J*,*Ks*-band photometry and polarimetry observations of 3C 66A from July 2008 to February 2010, using the TRISPEC instrument installed to the 1.5m Kanata telescope located at the Higashi-Hoiroshima Observatory. TRISPEC has a CCD and two InSb arrays, enabling photopolarimetric observations in one optical and two NIR band simultaneously (Watanabe et al. 2005). We obtained 278 photometry data and 208 polarimetry data of the V band, 180 photometry data of the J band, and 77 photometry data of the Ks band. A unit of the observing sequence consisted of successive exposures at 4 position angles of a half-wave plate; $0°, 45°, 22.5°$, and $67.5°$. The data reduction was performed under the standard procedure of CCD photometry. We performed the aperture photometry using `APPHOT` packaged in `PYRAF`, and the differential photometry with a comparison star taken in the same frame of 3C 66A. Its position is at R.A.=02:22:55.12 and Dec=+43:03:15.5 (J2000), and its magnitudes are V = 12.809, J=12.371, Ks=12.282(Gonzalez et al. 2001, Cutri et al. 2003). The data have been corrected for the Galactic extinction of $A(V)$=0.274 and $A(J)$=0.076. We confirmed that the instrumental polarization was smaller than 0.1% in the V band, using unpolarized standard stars. We hence applied no correction for it. The polarization angle (PA) is defined by the standard manner (measured from north to east), by calibrations with polarized stars, HD19820 and HD25443 (Wolff et al. 1996). Because the PA has an ambiguity of $\pm 180 \times n°$ (where n is an integer), we selected n which gives the least angle difference from the previous data, assuming that the PA would change smoothly.

Figure 1 shows time variations of flux and polarization in the optical and NIR band, together with the GeV gamma-ray light curve. Roughly speaking, there are several states according to the flux and polarization degree. Before JD = 2454830, the gamma-ray and optical flux are low on average, but a short flare was observed on JD = 2454750 in both the gamma-ray and optical band, which corresponds to the flare mentioned in Abdo et al. (2010d). Hereafter, we define this period as the period 1. In the period 1, optical properties violently varied and the gamma-ray flux seems to well correlate with the optical flux, color, and polarization degree (PD). After JD = 2454830, fast variations of the optical flux disappered (period 2). The polarization degree became relatively low with a slow variability and the PA is also constant. On JD = 2454830, the optical flux suddenly increased and the high-optical-flux state began without the change of PD.

During the period 2, the optical observations were poor, and thus we cannot study the correlation well. After JD 2455047, the continuous optical observations were available, and the PD became relatively high. Therefore, we distinguished this period as the period 3 from the period 2. After JD 2455151, the PD became lower and the color became redder (period 4). In the period 4, the optical flux was the highest and the gamma-ray flux was relatively higher than that in the period 3. A weak flare was seen on JD 2455190, associated with the decrease of the PD and a temporary shift of the PA by ∼40 deg.

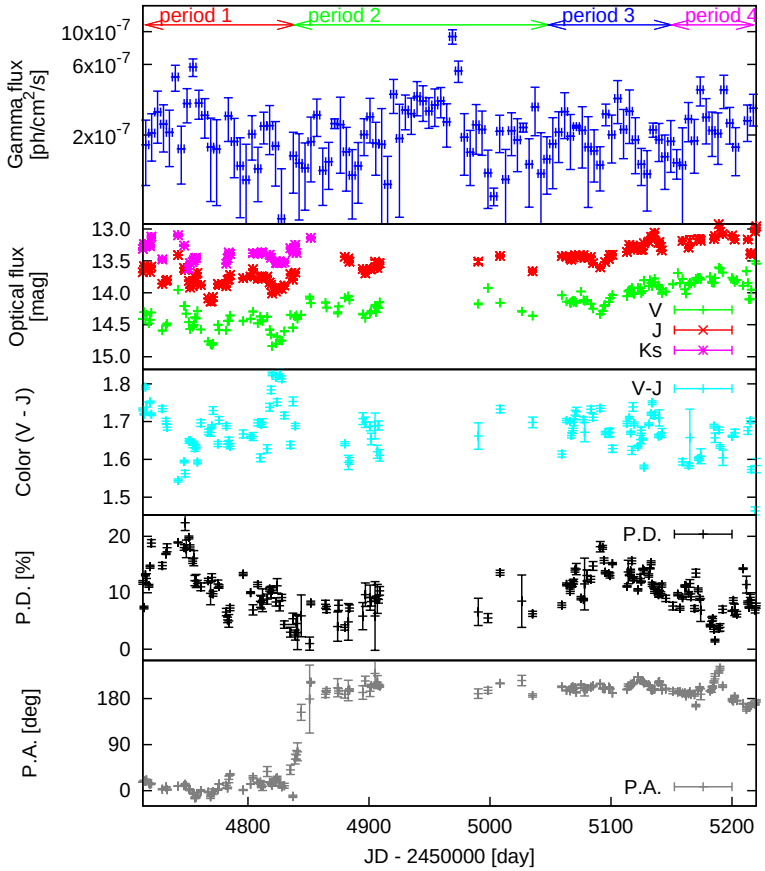

Fig. 1. Optical and GeV gamma-ray light curves of 3C 66A measured with the Kanata telescope and Fermi LAT. Top panel is the Gamma-ray light curve (100MeV–100GeV). The 2nd panel is the optical V, J, Ks-band flux in unit of magnitude. The 3rd panel is an optical color index (V band - J band). The 4th panel is a V-band polarization degree (PD) and bottom panel is its polarization angle (PA).

2.3. Correleation between Gamma-ray and Optical

Although the correlation is not clear for the whole data, the correlation is suggested in the period 1. This correlation in the period 1 was consistent with the results using other optical observational data (Abdo et al. 2010d). There is no clear correlation between the optical flux and PD. It is suggested that the optical flux correlates with the color in the period 1 and 2 in such a way that the optical flux is higher with the bluer color, so called a bluer-when-brighter trend.

When looking at only the flares, some additional correlations are found. In the period 1, the correlation between the optical flux and PD is seen at the flare on JD 2454750, but it is unclear besides this flare. This flare also causes the correlation between the gamma-ray flux and PD as described above. In the period 4, as described in the previous subsection, there is an anti-correlation between the optical flux and PD, together with the temporary change of PA, in the flare at JD 2455190.

The optical flux is different by a factor of 3–4 for the same gamma-ray flux among four periods. This indicates that the origin of the gamma-ray emission is not indentical to that of the optical emission. PD is systematically different among four periods. This behavior is due to a slow change of PD for the long-term variable component, and this trend is similar to that found for 3C454.3 (Sasada et al. 2010). Anti-correlation between the optical flux and PD is seen in the long term during the period 3 and 4, and this could be due to such a long-term variation. Apart from the bluer-when-brighter trend within each period, the relation of the optical flux and color is different among four periods. The bluer-when-brighter trend is also seen in the long term during the period 3 and 4. This is due to the long-term change of color as reported for 3C454.3 (Sasada et al. 2010). These implied at least two components with different variable time-scales in the optical band.

3. Discussion

It is known that the gamma-ray and optical variability of FSRQs often shows a clear correlation in the past observations, such as PKS 1510+089 (Abdo et al. 2010f), 3C 279 (Abdo et al. 2010e), PKS 1502+106 (Abdo et al. 10g), and 3C454.3 (Striani et al. 2010), and the spectral energy distribution (SED) in the wide energy band is better explained by the SSC+ERC model than the SSC model for FSRQs and LBLs (Abdo et al. 2010a). This result indicates that the radiation region of gamma-rays is the same as that of the optical band for FSRQs and LBLs. Our observations showed that there are two types of variations in which the correlation between gamma-ray and optical flux are clear or not. The correlation in the period 1 in 2008 was also reported in Abdo et al. (2010d), and the gamma-ray emission could be explained by the SSC+ERC model, and this is the first case for IBLs. On the other hand, the optical flux independently increased against the gamma-ray flux from the period 1 to 4, and no clear correlation between the optical and gamma-ray flux in the period 2, 3, and 4. Such a type of variations is for the first time found for 3C 66A, and there is no ever report that both types of correlations are found for other blazars.

When the averaged flux in the optical and gamma-ray band in the period 1 (2008) and period 4 (2009) are compared, the optical flux in the period 4 is about twice as that in the period 1 even though the gamma-ray flux is similar between the period 1 and 4. Abdo et al. (2010d) suggested that the Gamma-ray emission is dominated by the ERC in the period 1 (2008), based on the multiwavelength data. On the other hand, it is difficult to estimate how the ERC radiation contributes to the gamma-ray emission in the period 4 from only the optical and gamma-ray data used here. We thus assumed that the gamma-ray flux gives an upper limit of ERC radiation and then calculated the upper limit of energy density of external photons.

The period 1 is characterized by higher energy density of external photons and the correlation between flux and polarization degree is clearly seen. High energy density of external photons in 2008 indicates that the emission region locates near the nucleus where the disk photons are rich or the flux of external photons decreases. The faster flux variation in the optical band in 2008 than in 2009 prefers the former case. Since the magnetic field could align in the compact region, the correlation of PD with the optical and gamma-ray flux in the period 1 can also be explained. Bluer-when-brighter trends are found in the period 1 (2008). This can be explained by the input of fresh high energy electrons or the increase of the jet doppler factor.

On the other hand, the external photons in 2009 is estimated to be poor and then the emission region is far from the nucleus in 2009. The slow time variability in 2009 supports this scenario, and this causes a weak flux increase in the gamma-ray band against in the optical band. The brightening optical component in 2009 was associated with the bluer color, but the PD decreased as the flux increased. Such a behavior of the PD is also found in some blazars (Ikejiri et al. 2009), and could be explained by that there are two components of an underlying constant one and a short-term variable one and they have a different polarization direction (Uemura et al. 2010).

For some blazars, it is suggested that the emission region locates at $\sim 10^{19}$cm from the black hole (e.g.,PKS 1510-089, Marscher et al. 2010; 3C 279, Abdo et al. 2010e.). However, the emission region closer to the nucleus at $\sim 10^{17}$cm is also suggested (e.g., 3C 454.3, Abdo et al. 2010h). The location of emission region is discussed in several blazars but a unified view has not been obtained yet. From multiwavelength observations of a lot of blazars, it is suggested that the one-zone SSC model cannot explain the SED of some blazars (e.g. Abdo et al. 2009b). Our result indicates that there are several emission regions in the jet.

References

Abdo, A. A., et al., 2009a, ApJ, 707, 1310
Abdo, A. A., et al., 2009b, ApJL, 696, L150
Abdo, A. A., et al., 2010a, ApJ, 715, 429
Abdo, A. A., et al., 2010b, ApJS, 188, 405
Abdo, A. A., et al., 2010c, ApJS, 187, 460
Abdo, A. A., et al., 2010e, *Nature*, 463, 919
Abdo, A. A., et al., 2010f, ApJ, 721, 1425
Abdo, A. A., et al., 2010g, ApJ, 710, 810
Abdo, A. A., et al., 2010h, ApJ, 721, 1383
Abdo, A. A., et al., 2010i, ApJ, 710, 1271
Abdo, A. A., et al., 2011, ApJ 726, 43
Aleksic, J., et al., 2010, astro-ph/1010.0550
Atwood, W., B., et al., 2009, ApJ, 697, 1071
Bramel, D., A., et al., 2005, ApJ, 629, 108
Cutri., et al., 2003, 2MASS All Sky Catalog of Point Sources
Gonzarez-Perez, J., N., et al., 2001, ApJ, 122, 2055
Ikejiri, Y., et al., 2009, Proc. of 2009 Fermi Symposium, eConf Proceedings C0911022, arXiv:0912.3664
Marscher, A., P., et al., 2008, *Nature*, 452, 966
Marscher, A., P., et al., 2010., ApJ, 710, 126
Miller, J., S., et al., 1978, in *BL Lac Objects,*, 176
Sasada, M., et al., 2010, PASJ, 62, 645
Sikora, M., et al., 2008, ApJ, 675, 71
Striani, E., et al., 2010, ApJ, 718, 455
Uemura, M., et al., 2010, PASJ, 62, 69
Watanabe, M., et al., 2005, PASP, 117, 870
Wolff, M., J., et al., 1996, AJ, 111, 856